VALIDATION OF A SEA SURFACE MODEL FOR SIMULATIONS OF DYNAMIC MARITIME SAR IMAGES

Luis E. Yam, Jordi J. Mallorqui, Joan M. Rius

Remote Sensing Lab. (RSLab), Dept. of Signal Theory and Communication
Universitat Politècnica de Catalunya (UPC), Barcelona, Spain

ABSTRACT

Controllable maritime scenarios have become a central issue in the research of new applications of SAR imaging to vessel monitoring systems. Numerical tools such as GRECOSAR, a SAR simulator of complex targets, are able to provide suitable test-beds as long as the model of the targets (vessels) and the sea surface resemble to what is expected in real maritime scenes. This paper presents the validation of SAR simulated images from GRECOSAR while using a dynamic and multi-harmonic elevation model of the sea surface. The simulations are carried out for generic C- and X-band SAR sensors. The results of the co-polar channels are compared with K, lognormal, Weibull and Rayleigh distributions, which are commonly used to describe statistics of real SAR images of the sea surface. The results show that the clutter has statistics closer to the K and Weibull distributions, suggesting that the elevation model presented can provide a more realistic approach in simulating SAR images of maritime scenarios.

Index Terms— SAR, sea surface, simulation, k-distribution, GRECOSAR

1. INTRODUCTION

In recent years, great efforts have been aimed to develop reliable vessel monitoring systems based on SAR imaging. The attractiveness of these systems resides on its surveillance capability which is independent of weather conditions and sunlight, complementing existing monitoring technologies.

Nowadays, the main progress of this kind of monitoring systems resides on the vessel detection chain. Different techniques for single channel, polarimetric and interferometric detection have been successfully applied to achieve low false alarm rates [1-4]. In contrast, vessel classification still requires more improvement and research to achieve a similar performance.

Vessel classification is much more complicated in real scenarios. Vessels are complex targets whose signatures usually change as a function of the angle of observation and aberrations are commonly produced on the SAR images due to their motions [5]. Moreover, in the case of maritime SAR images, the complete control of the scenario or even ground truth is not always possible, which hinders implementation, testing and improvement of classification algorithms.

In this framework, the numerical tool GRECOSAR [5], developed by the Universitat Politècnica de Catalunya (UPC), has the capability of obtaining SAR signatures of complex targets. Thus, GRECOSAR can provide a controllable ground truth virtually for any scenario whose accuracy would depend on the level of detail of the models of the targets and the background. This numerical tool has already been used as a test-bed in the research of vessel classification techniques by using different 3D ship models and a simple two-harmonic modulated surface as the sea [5-7]. This simplified model of the sea surface provides SAR images with sea clutter whose statistics follows a Rayleigh distribution [7]. However, literature suggests that, in general, SAR images of the sea present clutter with statistics similar to the K-distribution [2,8].

A more realistic model of the sea surface would lead to simulate SAR images with clutter statistics closer to what is expected in real cases. In this paper we present the validation of simulated SAR images by using a dynamic and multi-harmonic elevation model of the sea surface. It provides a good trade-off between complexity and the general description of the waves on the surface, which makes it suitable for simulation environments [9]. This model considers several harmonics whose energy is given by the defined International Ship Structure Committee (ITTC) sea spectrum (a.k.a. modified Pierson-Moskowitz spectrum). Moreover, different directions of propagation are taken into account for these harmonics, resulting in a realistic elevation of the sea surface for modeling the maritime scenes (figure 1a).

The 3D model of the sea surface is validated through simulations in GRECOSAR in C- and X-band. We compare the statistics of the magnitude of sea clutter of the SLC image of the co-polar channels against four common distributions associated to real sea scenarios: K, lognormal, Weibull and Rayleigh.

In this paper, Section 2 is devoted to the mathematical model for the elevation of the sea surface. The simulations with GRECOSAR for C- and X-band are described in Section 3. In Section 4, the Kolmogorov-Smirnov (K-S)

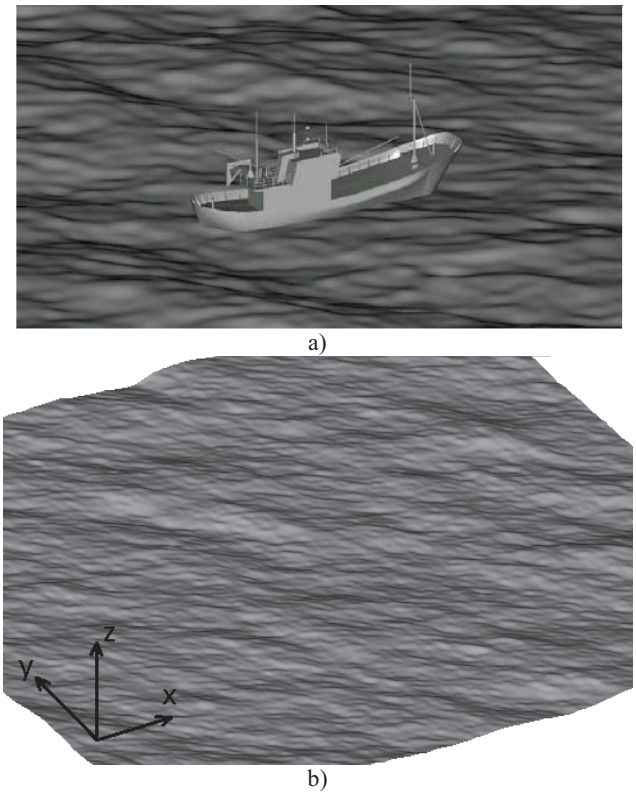

a)

b)

Figure 1. a) Detail of a maritime scene in GRECOSAR with the multi-harmonic model of the sea surface. b) Example of the multi-harmonic model of the sea surface used for the validation. Sea state (h_s=2.28 m and T_1=4.5 s)

statistic is used to compare the empirical cumulative distribution function (cdf) of the simulated images and the theoretical cdf of K, Rayleigh, lognormal and Weibull distributions.

2. MODEL OF THE SEA SURFACE ELEVATION

The model implemented for the sea surface elevation is based on the linear wave theory approach followed in ship motion control. From the hydrodynamic description of a fluid motion, and considering a travelling wave and infinite depth, the elevation of a regular wave (i.e. a harmonic component) is expressed as [10]:

$$\zeta(x,y,t) = \bar{\zeta}\sin(\omega t + \varepsilon - k(x\cos\chi + y\sin\chi)) \qquad (1)$$

where x and y are the Cartesian coordinates on the horizontal plane, $\bar{\zeta}$ is the amplitude of the wave, t is the time, ε is the initial phase, k is the wave number, ω is the circular wave frequency (related to the wave period T by $\omega = 2\pi/T$), and χ is the angle between the wave course and the positive axis x. Due to the random nature of ocean waves, elevation $\zeta(x,y,t)$ at a certain point (x,y) is considered a stochastic process. Moreover, this process is usually assumed to be stationary, homogeneous zero mean Gaussian, and characterized by the Power Spectral Density

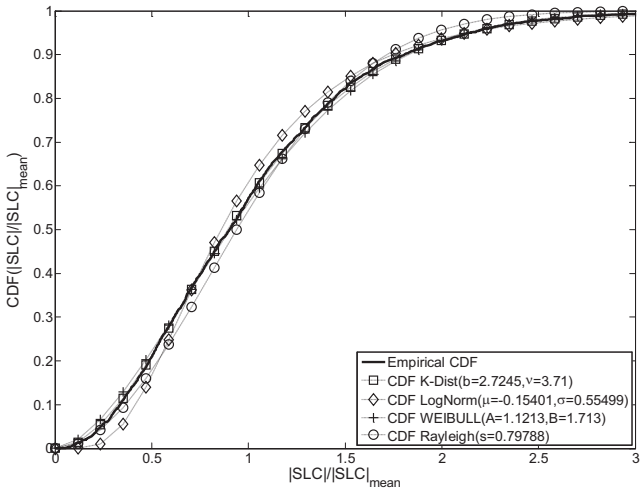

Figure 2. X-Band Sensor. Empirical cdf and theoretical cdf of K, Log-normal, Weibull and Rayleigh distributions. Data from the HH channel of the simulated SAR image (sea state 2).

(PSD), $S_{\zeta\zeta}(\omega)$ [10]. This PSD describes how the energy of the sea surface is distributed in the frequency domain. In our case, we adopt for $S_{\zeta\zeta}(\omega)$ the ITTC spectrum formulation for fully developed seas with no swell (a.k.a. modified Pierson-Moskowitz spectrum). For a gravity acceleration of $9.81\ m/s^2$, this spectrum is defined as:

$$S_{\zeta\zeta}(\omega) = \frac{A}{\omega^5}e^{-\frac{B}{\omega^4}} \qquad (2)$$

$$A = \frac{173h_s^2}{T_1^4}, B = \frac{691}{T_1^4} \qquad (3)$$

with h_s as the significant wave height, and T_1 as the average wave period. The particular scenario implemented in this study is a short-crested irregular sea. In general, this scenario is the usual case of the sea surface since it considers that waves propagate in different directions with one dominant direction. Hence, the PSD is a function of the frequency ω and the direction angle χ. This directional spectrum is represented as a product of two functions [10]:

$$S_{\zeta\zeta}(\omega,\chi) = S(\omega)M(\chi) \qquad (4)$$

$$M(\chi) = \begin{cases} \frac{2^{(2n-1)}n!(n-1)}{\pi(2n-1)!}\cos^{2n}(\chi-\chi_0), & |\chi-\chi_0| < \frac{\pi}{2} \\ 0 & otherwise \end{cases} \qquad (5)$$

where χ_0 is the dominant wave propagation and $M(\chi)$ is a spreading function (in our case, we use $n = 2$). Then, based on the statistical properties assumed for $\zeta(x,y,t)$, the simulation of the sea surface elevation at a point (x,y) can be represented as a sum of regular waves of different amplitudes [10]:

$$\zeta(x,y,t) = \sum_{n=1}^{N}\sum_{m=1}^{M} \bar{\zeta}_{n,m} \sin(\omega^* t + \varepsilon_{n,m} - k_n(x\cos\chi_m + y\sin\chi_m)) \quad (6)$$

$$\bar{\zeta}_{n,m} = \sqrt{2S_{\zeta\zeta}(\omega^*,\chi^*)\Delta\omega\Delta\chi} \quad (7)$$

with ω^* and χ^* taken randomly in each of the intervarls $\left[\omega_n - \frac{\Delta\omega}{2}, \omega_n + \frac{\Delta\omega}{2}\right]$ and $\left[\chi_m - \frac{\Delta\chi}{2}, \chi_m + \frac{\Delta\chi}{2}\right]$ respectively. Figure 1a depicts an example of 3D model of the surface with dimensions of 200 x 200 m and a moderate sea state (code 4).

3. SEA CLUTTER SIMULATIONS

Equation (6) was implemented as an extension of the current sea models used in GRECOSAR to simulate the dynamic sea surface of the sea. The elevation is computed on the grid nodes of a limited flat plane of 200x200 meters. In a similar way to [6], this plane was discretized in triangular dielectric facets of 0.15 m length with the corresponding dielectric permittivity for the working frequency. Moreover, we consider the number of harmonics and directions of propagation fixed as *N=40* and *M=10*, respectively. The set of simulations contemplates smooth (wavelets) to moderate sea states in the case of well-developed wind waves of open sea (i.e. sea states codes 2 – 4). Table 1 shows the values of h_s and T_1 considered for each sea state in our simulations.

GRECOSAR's flexibility allows the use of different SAR sensors. We carry out the simulations with generic C- and X-band sensors with azimuth-range (AxR) resolution of 4 x 10 m and 2 x 1.3 m respectively. Table 2 summarizes the main parameters of both sensors.

4. VALIDATION OF THE SEA CLUTTER STATISTICS

Different models have been proposed in the literature to describe the statistics of the clutter of the sea surface. Popular distributions such as the K, Rayleigh, lognormal and Weibull are suggested as good descriptors of real clutter in marine scenarios [2,8]. Hence, we consider these four distributions in order to test their fitting to the magnitude of simulated SLC single-pol SAR images normalized to their mean value, i.e. $E = |SLC|/|SLC_{mean}|$. Additionally, their shape parameters are computed numerically based on the expressions in [8] for their first and second moment. Figure 2 shows an example of the empirical and the theoretical cdfs computed from the HH channel of the simulated SAR image of the X-band sensor.

In order to evaluate the fitting of a theoretical distribution to the empirical one (i.e. the simulated SLC image), the parameter adopted is D_n, the Kolmogorov-Smirnov (K-S) distance which is based on the separation between both cdfs. For a sample of size n:

TABLE 1
Values of h_s and T_1 considered for each sea state in simulations.

Sea State	h_s[m]	T_1[s]
2	0.914	2.5
3	1.524	3.5
4	2.286	4.5

TABLE 2
Main parameters of generic C- and X-band sensors deployed in GRECOSAR's simulations.

Sensor	Freq [GHz]	Incidence angle [°]	PRF	Chirp BW [MHz]	Pulse duration τ (μs)
C-Band	5.3	23	1700	15.5	37.12
X-band	9.65	20	3736	116	28

$$D_n = \sqrt{n}\,\sup_E |F(E) - F_e(E)| \quad (8)$$

where $F(E)$ and $F_e(E)$ denote the theoretical and empirical cdf, respectively. Therefore, a small value of D_n indicates that the shape of the theoretical distribution follows the empirical one. In fact, with $D_n < 1.36$, it can be considered that $F_e(E)$ is described by $F(E)$ with a level of significance of 5%. However, since the parameters of the theoretical distribution have been estimated from the data, the K-S test is only approximate [11].

Table 3 shows the values of the parameter D_n for each of the four distributions with different sea states and sensors. In the case of the C-band sensor, all the ROIs considered contain more than 400 samples. For the X-band sensor, all ROIs contain more than 2000 samples. Additionally, another set of simulations were carried out with the same sensor but changing their incidence angle to 40°. Table 4 shows the results of this second set of simulations.

The results in both tables show that the magnitude E of the ROIs, in general, is similar to at least one of the four distributions, the k distribution being the closest one in most of the cases. This suggests that the elevation model deployed in the simulation of the sea surface can produce SLC images whose statistics are similar to those reported for real SAR sea surface images.

5. CONCLUSIONS

The elevation model implemented for the sea surface is based on the superposition of regular waves with different directions and amplitudes. We used the ITTC spectrum formulation for fully developed seas with no swell to assign the energy of each harmonic in the model. In this way, a more realistic sea surface was implemented for marine environments in GRECOSAR, the SAR simulator of complex targets used in this paper.

For the validation of the model, the cdfs of the magnitude of the simulated co-polar channels were compared to theoretical cdfs associated with real sea clutter. Four distributions have been considered: K, lognormal, Weibull and Rayleigh. Their parameters have been

TABLE 3
Values of parameter D_n for different sea states; C- and X-band sensors with incidence angle of 23° and 20°, respectively.

Sea State	Sensor	D_n			
		K	Lognormal	Weibull	Rayleigh
2	HH-C	0.54	1.24	0.69	1.01
2	VV-C	0.28	1.36	0.46	0.75
2	HH-X	0.56	3.23	1.28	2.57
2	VV-X	0.55	3.33	1.47	3.33
3	HH-C	0.43	1.5	0.5	0.91
3	VV-C	0.42	1.51	0.57	0.99
3	HH-X	2.69	1.88	3.48	3.41
3	VV-X	2.74	2.06	3.72	4.01
4	HH-C	1.05	1.36	0.64	0.85
4	VV-C	1.07	1.39	0.61	0.88
4	HH-X	0.55	3.23	0.937	1.52
4	VV-X	0.41	3.51	1.11	2.01

TABLE 4
Values of parameter D_n for different sea states; both C- and X-band sensors with incidence angle of 40°.

Sea State	Sensor	D_n			
		K	Lognormal	Weibull	Rayleigh
2	HH-C	0.64	1.72	0.59	1.07
2	VV-C	0.48	1.69	0.49	0.71
2	HH-X	0.76	5.07	1.42	3.97
2	VV-X	0.65	5.45	0.96	3.09
3	HH-C	0.43	1.75	0.60	0.93
3	VV-C	0.55	1.71	0.64	0.56
3	HH-X	0.52	4.79	1.45	3.35
3	VV-X	0.81	4.47	1.82	3.61
4	HH-C	0.72	1.32	1.12	1.62
4	VV-C	0.62	1.57	0.84	1.22
4	HH-X	0.51	5.29	1.46	3.36
4	VV-X	1.19	4.12	2.64	5.24

computed numerically from ROIs of the simulated SAR image.

The Kolmogorov-Smirnov distance was used to identify the distribution that better adjust the data. In general, for both sensors, the K and Weibull distributions were the closest to the simulated data, as is also reported in literature. Additionally, the analysis was extended to a second set of simulations in which the incidence angles of the sensors were fixed to 40°, and similar tendencies were observed.

The results are encouraging for the use of the elevation model presented in this paper for future studies of vessel classification with GRECOSAR since it can provide a more realistic approach in simulating SAR images of maritime scenarios.

6. ACKNOWLEDGEMENTS

This research work has been supported by the Spanish MICINN under project TEC2011-28201-C02-01 and the European Community under project NEREIDS (FP7-SPACE-2010-1 contract 263468).

7. REFERENCES

[1] D. J. Crisp, "The state-of-the-art in ship detection in synthetic apertureradar imagery," *Intell., Surveillance and Reconnaissance Div., Inf. Sci.Lab., Def., Sci. Technol. Org*., Edinburgh, S.A., Australia, Res.Rep. DSTO-RR-0272, May 2004.

[2] G. Ferrara, M. Migliaccio, F. Nunziata, A. Sorrentino, "Generalized-K (GK)-Based Observation of Metallic Objects at Sea in Full-Resolution Synthetic Aperture Radar (SAR) Data: A Multipolarization Study," *Oceanic Engineering, IEEE Journal of*, vol.36, no.2, pp.195-204, April 2011.

[4] S. Suchandt, H. Runge, U. Steinbrecher, "Ship detection and measurement using the TerraSAR-X dual-receive antenna mode," *Geoscience and Remote Sensing Symposium (IGARSS)*, 2010 IEEE International , vol., no., pp.2860-2863, 25-30 July 2010.

[5] G. Margarit, J.J. Mallorqui, J. M. Rius, J. Sanz-Marcos, "On the Usage of GRECOSAR, an Orbital Polarimetric SAR Simulator of Complex Targets, to Vessel Classification Studies," *Geoscience and Remote Sensing, IEEE Transactions on*, vol.44, no.12, pp.3517-3526, Dec. 2006.

[6] G. Margarit; J.J. Mallorqui, "Study of Sea Clutter Influence in Ship Classification Algorithms based on Polarimetric SAR Inteferometry," *Synthetic Aperture Radar (EUSAR)*, 2008 7th European Conference on, pp. 1-4, June 2008.

[7] G. Margarit, J.J. Mallorqui, J. Fortuny-Guasch, C. Lopez-Martinez, "Exploitation of Ship Scattering in Polarimetric SAR for an Improved Classification Under High Clutter Conditions," *Geoscience and Remote Sensing, IEEE Transactions on*, vol.47, no.4, pp.1224-1235, April 2009.

[8] K.D. Ward, R. J.A. Tough, and S. Watts, *Sea clutter: scattering, the K-distribution and radar performance*, ITC, 2006.

[9] Perez, T., *Ship motion control: Course keeping and roll stabilization using rudder and fins*, Springer, 2005.

[10] E. Omerdic, D. Toal, "Modelling of waves and ocean currents for real-time simulation of ocean dynamics", *OCEANS 2007 – Europe*, vol., no., pp.1-6, 18-21 June 2007.

[11] Schay, G., *Introduction to Probability with Statistical Applications*, Springer, 2007.